Available online at www.sciencedirect.com
ScienceDirect
Lithos 91 (2006) 173–190
LITHOS
www.elsevier.com/locate/lithos

Peralkaline silicate lavas at Oldoinyo Lengai, Tanzania

Jurgis Klaudius *, Jörg Keller

Institut für Mineralogie, Petrologie und Geochemie, Albert-Ludwigs-Universität Freiburg, Albertstr. 23 B; 79104 Freiburg, Germany

Received 3 September 2005; accepted 13 March 2006
Available online 16 June 2006

Abstract

A detailed study of Oldoinyo Lengai has led to the recognition of two major cone-building stages. An early, predominantly phonolitic stage, Lengai I, forms the southern cone. The recent nephelinitic Lengai II developed following a major sector collapse event over Lengai I. Petrography of Lengai II lavas show that nephelinite is combeite- and wollastonite-bearing. All Oldoinyo Lengai lavas are peralkaline and highly evolved in terms of low Mg#, Ni and Cr values. Within the unique Lengai II combeite–wollastonite–nephelinite (CWN) peralkalinity increases with time to extreme values (Na+K)/Al=2.36. Mineralogical expression of peralkalinity is the presence of combeite and Na-rich clinopyroxene. In addition, exceptionally high Fe_2O_3 (up to 10.28 wt.%) in nepheline is an indicator for alumina deficiency. Combeite also shows high Fe^{3+}. Phonolite and CWN of Lengai I and Lengai II show similarly enriched LILE and LREE values and generally parallel patterns in PM normalized and REE plots.

Keywords: Oldoinyo Lengai; Natrocarbonatite; Peralkaline silicate lavas; Phonolite; Combeite wollastonite nephelinite

1. Introduction

Oldoinyo Lengai is the only active carbonatite volcano on Earth. The 2951 m high (Anderson, 2005) stratocone rises steeply 2200 m from the rift plain of the Gregory Rift in northern Tanzania. The volcano consists predominantly of nephelinite and phonolite (Donaldson et al., 1987; Dawson, 1989). Geochemically, these lavas are alkaline and reach high levels of peralkalinity (molar (Na+K)/Al) with an unusual mineralogy that includes combeite (ideal formula $Ca_2Na_2(Si_3O_9)$) in the most recent combeite–wollastonite nephelinites, CWN (Peterson, 1989a; Dawson et al., 1989; Keller and Krafft, 1990; Dawson, 1998).

Several groups of peralkaline magma types are involved in the evolution of Oldoinyo Lengai. Specifically, these are olivine melilitite, phonolite, nephelinite and natrocarbonatite. Phonolite and nephelinite constitute the cone-building silicate pyroclastics and lavas (Dawson, 1962; Donaldson et al., 1987). Olivine melilitite pyroclastics and lavas form parasitic cones and craters (Keller et al., 2006-this volume), whereas natrocarbonatite is restricted to the active crater of Oldoinyo Lengai. A liquid immiscibility relationship has been suggested between peralkaline, evolved, carbonated and silicic compositions and the natrocarbonatite lavas at Lengai (Williams et al., 1986; Peterson, 1989b, 1990; Lee and Wyllie, 1994; Keller and Spettel, 1995; Church and Jones, 1995; Bell and Dawson, 1995; Kjarsgaard et al., 1995; Dawson et al., 1996; Simonetti et al., 1997; Dawson, 1998; Lee and Wyllie, 1998). However, there is still controversy about the exact composition of conjugate silicate–carbonatite liquids

* Corresponding author. Tel.: +49 761 203 6414; fax: +49 761 203 6407.
E-mail address: klaudius@uni-freiburg.de (J. Klaudius).

0024-4937/$ - see front matter © 2006 Elsevier B.V. All rights reserved.
doi:10.1016/j.lithos.2006.03.017

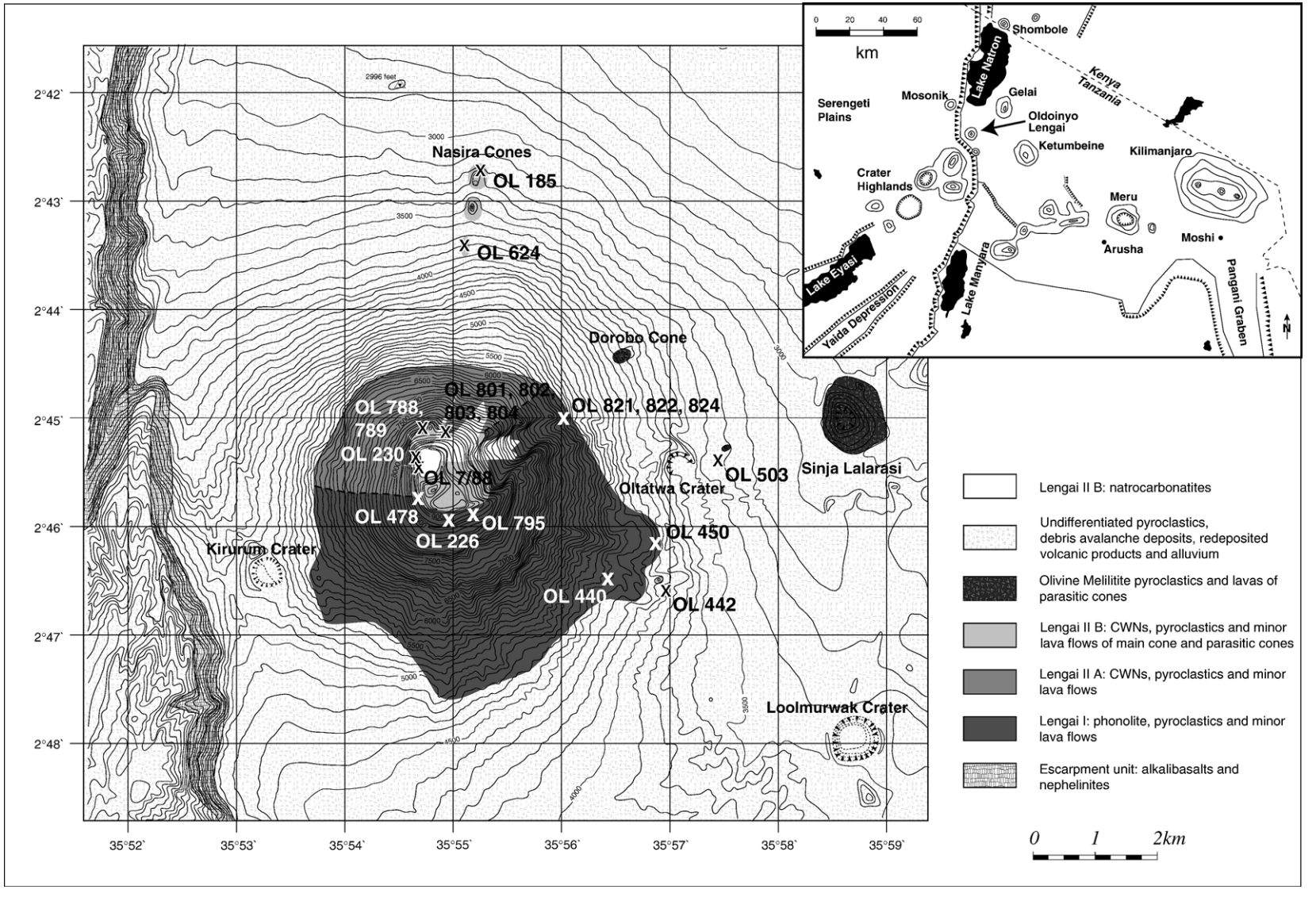

Fig. 1. Geological map of Oldoinyo Lengai showing the distribution of silicate and carbonatite lavas. Topography adapted from sheet 39/4, Tanzanian topographic map series Y 742, altitude in feet, UTM-Grid ARC1960. Insert panel shows northern Tanzanian sector of EARS (after Dawson, 1992).

and the timing and conditions of separation of these two melts.

High-Mg olivine nephelinite and olivine melilitite have been proposed as parental melts for the evolution of the Lengai suite (Peterson and Kjarsgaard, 1995; Dawson, 1998; Keller et al., 2006-this volume). According to Peterson (1989a), at Shombole volcano, Kenya, olivine nephelinites evolve by fractionation towards mildly peralkaline nephelinites and associated calciocarbonatites, whereas at Lengai the fractionation is directed towards highly peralkaline combeite–wollastonite nephelinites (CWN) from an olivine melilitite parental magma. The so far only postulated high-Mg melilititic parent has been identified at the tuff and scoria cones in the northern and eastern foreland of Lengai and Kerimasi (Keller et al., 2006-this volume).

This paper presents detailed geochemistry and mineralogy of lavas preceding (phonolite) and alternating (CWN) with the carbonatite activity of Oldoinyo Lengai and describes their spatial distribution (Fig. 1) with the main emphasis on CWN.

2. Setting, stratigraphy and spatial distribution of units

Oldoinyo Lengai is located in the eastern branch of the East African Rift System, south of Lake Natron (Fig. 1) and close to the ca. 400 m high Natron Escarpment of the Gregory Rift, which formed 1.2 Ma ago (Foster et al., 1997). Volcanic activity in the Gregory Rift started about 10 Ma ago (Macdonald et al., 2001) in its northern part and propagated to the SW to the site of recent volcanic activity of Oldoinyo Lengai on the southern edge of the Lake Natron basin. The volcano is located at the boundary between the Archaean Tanzanian Craton and the reworked craton margin that was overthrust and buried by rocks of the Mozambique mobile belt (Smith and Mosley, 1993; Macdonald et al., 2001). The timing of the onset of volcanic activity at Oldoinyo Lengai is poorly constrained with an age of 0.37 Ma for pyroclastics underlying the "yellow tuffs and agglomerates" (Bagdasaryan et al., 1973).

Oldoinyo Lengai is mostly explosive and consists of pyroclastic deposits. In the middle and upper portions of the edifice, lava flows are interbedded with the pyroclastics and reach the lower slopes at the eastern and southern flanks. Systematic sampling of cone-lavas forms the basis for the geochemistry presented in this paper.

Dawson (1962) first established a stratigraphy. As major structural units we define:

Lengai I: phonolite tuffs and phonolite lavas
Lengai II A: nephelinite tuffs and nephelinite lavas
Lengai II B: nephelinite tuffs, nephelinite lavas, gray melilite-bearing nephelinite tuffs and carbonatite tuffs and lavas of the active northern crater.

Phonolites are dominant in the early southern cone of Lengai I (Fig. 1), while nephelinites of Lengai II characterize the pyroclastics and lavas of the northern cone. Primary deposits of Lengai II A occupy the middle part of the northern cone, whereas the Lengai II B unit forms the upper cone including the summit area. A buried sector collapse scarp separates Lengai I and Lengai II (Fig. 2). This means that Lengai II formed

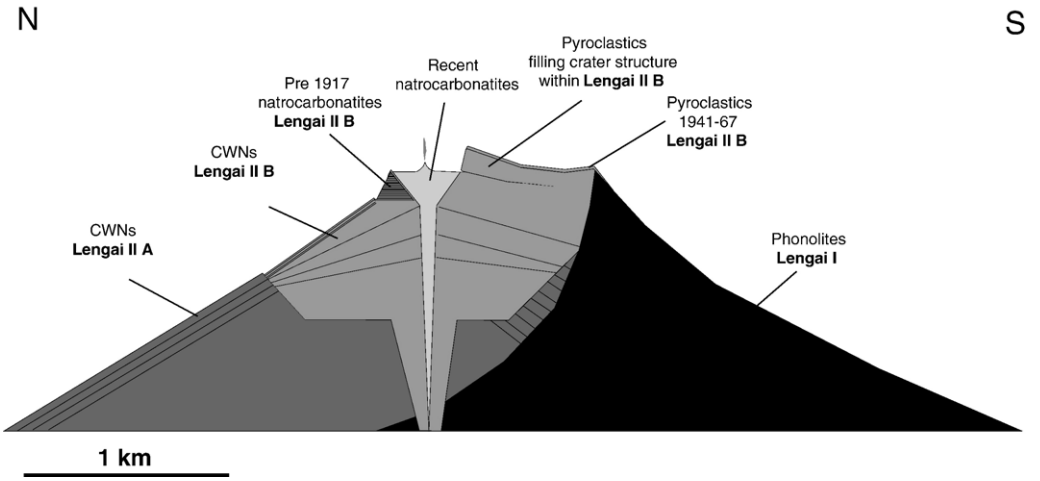

Fig. 2. Cross section of the Oldoinyo Lengai upper cone showing geometry and stratigraphic relations of units Lengai I and Lengai II.

after a major sector collapse event, which affected approximately 18% of the recent cone volume at around 10 ka ago (Klaudius and Keller, 2004). Lengai II A is separated from Lengai II B by a crater-rim unconformity visible at the upper northern flank. Most of the summit area is covered by gray colored CWN and melilite-bearing CWN pyroclastics of recent explosive eruptions (1917, 1940 and 1966/67), which consist of agglomerates, spherical lapilli, crystal lapilli and ash.

Peralkaline pyroclastics are strongly susceptible to alteration and show sodium loss compared to lavas of the same mineralogy. Melilite-bearing CWN-lavas on which accurate analysis could be performed have not been found at the cone of Oldoinyo Lengai. Only the northern most of the Nasira parasitic cones, located on the lower northern slope, produced juvenile scoria and bombs, which show only minor alteration features and are suitable for whole rock geochemical analysis. From the north to the south, the Nasira parasitic cones are two Strombolian scoria cones and one eruption fissure. They are aligned along a N–S striking lineament. The northern cone is subdivided into two eruptive stages. Its first stage produced CWN as the other Nasiras, whereas its second stage produced melilite-bearing CWN. Stratigraphy indicates that the Nasira parasitic cones and the olivine melilititic Dorobo cone on the lower eastern slope are closely related to the Lengai II activity.

Redeposited volcanic products (lahar deposits, debris avalanche deposits and alluvium) and interbedded tuffs of Lengai II dominate the lower parts of the volcanic edifice. Olivine melilitites and olivine nephelinites form parasitic and excentric vents on the northern and eastern slopes and foreland of Oldoinyo Lengai and are discussed in Keller et al. (2006-this volume).

Lengai I forms approximately 60% of the volcano's volume, Lengai II ~35% and carbonatites are subordinate with less than 5%.

3. Analytical methods

Whole rock analyses were carried out by XRF with a Philips PW 2404 instrument at the Institut für Mineralogie, Petrologie und Geochemie at Freiburg. Fused Li tetraborate pellets (1g sample and 4g flux) for major elements, pressed powder pellets (4 g sample and 1 g wax) for trace elements, were calibrated against international reference samples. Trace element concentrations and REE (Tables 1 and 2) were analyzed by ICP-MS at CRPG-CNRS (SARM) at Nancy, France. Analytical precision ranges from <5% to <10% depending on the concentration of the specific trace element.

Compositions of rock forming minerals (nepheline, clinopyroxene and combeite) were determined by wavelength-dispersive spectrometry (WDS) using a Cameca SX-100 electron microprobe at the Institut für Mineralogie, Petrologie und Geochemie (Freiburg University). The microprobe was operated at 15 kV, 20 nA for nepheline and clinopyroxene and 8 nA for combeite with spot sizes from 1 μm to 5 μm for nepheline and clinopyroxene and 20 μm for combeite. Well-characterized minerals and synthetic materials were used as standards. Data were reduced using the PAP routine (Pouchou and Pichoir, 1991).

For identification of minerals in lava samples, optical microscopy and backscattered electron images were used. The threshold between phenocrysts and microphenocrysts was set at 1 mm.

4. Petrography of Oldoinyo Lengai lavas

The list of sampled lavas and their localities from all cone-building units is given in Table 3 and marked in Fig. 1. Variations of the mineral associations in the lava suites are given in Fig. 3. The lavas are porphyritic and show a wide range in their degree of crystallization. The estimated proportion of phenocrysts and microphenocrysts varies from 30% in OL788 CWN to 90% in OL804 CWN (Fig. 4f). Glassy groundmass, with microlites, is a common constituent. Abundant vesicles are filled with zeolites and/or calcite. The lavas are black if the matrix is glassy, green if the matrix is microcrystalline and yellow if the matrix is altered. Nepheline and clinopyroxene occur as phenocrysts, microphenocrysts and groundmass phases in all lavas, whereas sanidine (Fig. 4e) and sodalite are restricted to phonolite. Apatite and magnetite are common groundmass phases in all lava samples. Ti-garnet (melanite–schorlomite), wollastonite and combeite phenocrysts are restricted to CWN and melilite-bearing CWN.

Within Lengai II lavas (CWN), the modal amount of clinopyroxene and Ti-garnet decreases with increasing total alkali contents and peralkalinity. The proportions of wollastonite and combeite may vary, but our systematic sampling and microscopic study shows that all Lengai II lavas are combeite- *and* wollastonite-bearing. In addition, evolved euhedral melilite appears as a major phenocryst phase in lava block OL247 of a monolithologic tuff breccia in the Dorobo canyon (Wiedenmann, 2004) and in OL184, juvenile bombs from the northernmost Nasira cone.

Table 1
Major and trace element analyses of Oldoinyo Lengai lavas

Cone-unit	I	I	I	I	I	I	I	I	I	I	IIA	IIA	IIA	IIB	IIB	IIB	IIB	IIB	IIB	IIB Nasira cones	II	II Nasira cones
Sample	OL 821	OL 822	OL 824	OL 442	OL 450	OL 478	OL 503	OL 226	OL 440	OL 795	OL 801	OL 803	OL 789	OL 7/88	OL 230	OL 788	OL 802	OL 804	OL 806	OL 624	OL 247	OL184
Rock type	phon	phon	phon	phon	phon	phon	phon	phon	phon	phon-neph	CWN	CWN	CWN	CWN	CWN	CWN	CWN	CWN	CWN	CWN	mel-CWN	mel-CWN
wt.%																						
SiO_2	51.93	50.01	48.54	51.07	52.91	50.52	49.34	51.89	47.94	44.98	44.97	46.32	45.45	43.50	45.04	44.58	43.33	45.51	44.78	43.40	41.79	40.15
TiO_2	0.77	0.85	1.18	1.01	0.98	0.93	1.56	0.98	0.99	1.20	0.81	1.16	1.10	0.95	1.00	1.06	0.95	0.96	0.99	1.35	1.59	1.60
Al_2O_3	18.18	18.73	16.70	18.48	18.94	18.15	17.67	19.05	17.69	17.62	17.12	15.77	14.79	13.89	13.15	13.51	12.80	12.37	17.62	12.29	14.20	12.26
Fe_2O_3	*5.59	*6.03	*7.85	*5.67	*5.79	*6.53	*7.53	*5.90	*7.06	*7.43	*7.43	*8.13	*9.12	5.45	5.95	*9.77	*9.59	*10.44	*7.44	*11.08	*5.01	11.27
FeO														2.96	3.50							4.41
MnO	0.20	0.21	0.24	0.18	0.18	0.21	0.22	0.19	0.23	0.23	0.28	0.29	0.32	0.33	0.39	0.35	0.37	0.41	0.23	0.41	0.31	0.39
MgO	0.75	0.83	1.12	0.85	0.74	0.93	1.28	0.80	0.81	1.20	0.69	1.18	1.09	0.90	0.71	0.93	0.78	0.64	0.83	1.28	1.95	1.91
CaO	3.84	4.39	5.98	4.89	3.40	5.09	5.45	3.91	6.05	7.61	6.69	8.29	9.31	10.97	8.46	7.44	8.10	6.58	7.48	8.83	11.12	12.86
Na_2O	9.29	11.17	10.02	10.00	9.95	9.56	10.35	9.31	9.78	10.35	11.87	10.87	9.65	12.00	11.85	12.71	14.64	14.09	11.46	12.39	10.67	8.29
K_2O	5.57	4.69	4.68	4.53	4.91	4.77	4.46	5.04	5.29	4.79	5.33	3.84	4.56	4.87	5.39	5.42	5.64	5.27	4.80	5.64	4.70	4.53
P_2O_5	0.42	0.30	0.27	0.58	0.26	0.35	0.38	0.20	0.23	0.39	0.26	0.50	0.42	0.65	0.37	0.42	0.36	0.31	0.28	0.61	0.89	0.94
LOI	2.72	1.94	2.60	1.19	1.01	2.61	0.52	2.39	3.55	3.49	3.86	2.84	3.15	2.40	3.33	1.66	1.72	1.65	3.5	0.56	2.79	3.94
Total	99.26	99.15	99.18	98.45	99.07	99.65	98.76	99.65	99.62	99.29	99.31	99.19	98.96	98.87	100.12	97.85	98.28	98.23	99.41	97.84	94.42	98.14
Mg#	23.17	23.62	24.28	25.20	22.31	24.25	27.64	23.35	20.50	26.60	17.27	24.59	21.17	18.80	13.96	17.62	15.45	12.11	20.04	20.61	30.66	27.58
AI	1.17	1.25	1.29	1.16	1.14	1.15	1.24	1.09	1.23	1.26	1.48	1.40	1.41	1.80	1.93	1.98	2.36	2.33	1.36	2.15	1.59	1.51
ppm	x	$	x	x	x	x	x	$	x	x	x	$	$	#	$	$	x	$	x	x	$	x
Rb	104	79	73	87	95	100	81	143.9	106	98	99	91	95	110	122	110	116	134	81	107	75	85
Sr	1777	1875	1695	2182	1700	1196	2068	1789	2026	2133	2543	2082	2451	2325	3038	2167	2912	2865	2154	1947	2215	2436
Ba	1376	1532	1415	1669	1523	1244	1614	1676	1440	1135	2152	1612	1704	1560	2417	1970	2424	2654	1323	1564	1431	1779
Pb	30	28	25	87	31	25	23	33	29	24	32	31	20	n.a.	51	41	40	53	23	35	24	33
Y	38	35	37	45	39	43	41	33	47	42	49	49	28	46	36	29	42	30	35	42	29	56
Nb	174	188	169	166	164	172	183	190	151	133	181	194	174	295	288	299	269	399	155	264	190	238
Zr	552	683	518	450	505	497	511	702	532	443	836	944	700	800	815	843	753	1041	439	842	589	794
Hf	12	11.53	12	11	11	11	13	11.36	12	9	16	13.51	10.32	12.4	12.61	10.63	15	12.34	9	16	9.47	15
V	59	78	62	59	55	90	120	73	124	123	91	171	203	215	138	184	133	179	111	216	262	225
Ni	b.d.	4.8	b.d.	b.d.	b.d.	b.d.	b.d.	4.9	b.d.	b.d.	b.d.	5.4	4.6	b.d.	4.8	7	b.d.	b.d.	b.d.	b.d.	6.3	b.d.
Cr	4	11	b.d.	18	10	4	4	8	17	b.d.	10	7	7	10	b.d.	5	b.d.	5	b.d.	20	6	b.d.
Co	5	6	5	7	7	7	9	6	7	8	7	9	10	n.a.	12	11	9	12	6	12	15	17
Cu	8	8	5	29	7	10	7	7	8	12	15	42	19	n.a.	37	43	31	41	9	52	40	75
Zn	142	165	148	131	132	160	145	159	178	152	203	202	218	260	313	271	270	346	170	283	190	248
Ga	31	33.1	29	26	95	29	27	33.6	27	25	34	31.4	32.2	36	42.1	38	31	44.4	27	36	29.5	23
Th	26	26.6	25	26	27	27	24	30.2	17	15	9	9.5	4.4	18	20.6	14.8	15	21.4	18	8	4.9	8
U	5	10.1	10	5	5	b.d.	6	5.5	5	5	8	7	3.2	9	10.3	7.8	8	10.6	5	6	3.4	6
Ta	b.d.	6.30	b.d.	7	8	b.d.	7	6.81	b.d.	b.d.	b.d.	3.08	2.02	5	5.51	4.92	5	6.03	b.d.	b.d.	3.26	b.d.

Major elements by XRF; ∗total iron; Mg#(0.15)=100 Mg/(Mg+Fe^{2+}); (Fe_2O_3/FeO=0.15); AI=peralkalinity index=(Na+K)/Al; x=trace elements by XRF; #=trace elements by INAA; $=trace elements by ICPMS; b.d. =below detection limit; n.a. =not analysed; Data for OL 7/88 from Keller and Spettel (1995).

Table 2
Rare earth element data and additional trace elements of Oldoinyo Lengai lavas

Cone unit	I	I	II A	II A	II B	II B	II B	II
Sample	OL226	OL822	OL803	OL789	OL788	OL804	OL230	OL247
Rock type	phon	phon	CWN	CWN	CWN	CWN	CWN	mel-CWN
ppm								
La	134	140	106	67	148	202	215	84
Ce	224	236	151	89	209	276	296	119
Pr	21.7	23.1	14.3	8.2	19.2	25.2	26.6	11.3
Nd	69.7	75.8	47.9	27.1	60.0	75.0	82.6	37.1
Sm	10.6	11.3	9.3	4.9	8.7	10.0	11.8	6.4
Eu	3.1	3.4	3.1	1.7	2.6	2.8	3.4	2.1
Gd	8.0	8.7	9.1	4.9	6.9	7.4	9.0	5.9
Tb	1.12	1.20	1.38	0.73	0.92	0.95	1.23	0.85
Dy	6.03	6.49	7.99	4.21	4.78	4.68	6.21	4.67
Ho	1.10	1.16	1.53	0.79	0.83	0.81	1.12	0.85
Er	3.00	3.15	4.22	2.24	2.29	2.27	2.98	2.31
Tm	0.43	0.46	0.62	0.32	0.34	0.34	0.44	0.33
Yb	2.78	2.90	3.08	2.23	2.21	2.28	2.87	2.06
Lu	0.42	0.43	0.56	0.35	0.35	0.35	0.43	0.31
Sum REE	485.39	513.94	360.43	213.45	466.27	610.30	659.80	277.21
As	1	b.d.	3	1	5	4	4	3
Be	7.7	8.2	11.0	10.0	14.4	20.0	17.4	8.6
Cd	0.70	0.56	1.08	0.60	3.72	1.17	1.08	0.74
Ge	1.06	1.13	1.12	0.99	0.96	0.98	0.90	0.97
Mo	2.5	2.3	1.5	1.0	4.9	2.6	3.1	3.0
W	2.2	2.4	1.6	0.5	2.8	1.8	1.8	1.6
Sn	2.0	2.0	4.4	3.0	3.1	2.6	2.7	2.9

Data obtained by ICPMS. b.d. = below detection limit.

Table 3
Sample list of Oldoinyo Lengai lavas

Sample	Cone unit	Rock type	Sample locality	Coordinates (GPS-ARC 1960)	
				S	E
OL 821	Lengai I	Phonolite	Lower E-flank, E-Chasm	2°45.046	35°56.058
OL 822	Lengai I	Phonolite	Lower E-flank, E-Chasm	2°45.046	35°56.058
OL 824	Lengai I	Phonolite	Lower E-flank, E-Chasm	2°45.082	35°55.975
OL 442	Lengai I	Phonolite	Lower SE-flank	2°46.530	35°56.882
OL 450	Lengai I	Phonolite	Lower E-flank	2°46.288	35°56.878
OL 478	Lengai I	Phonolite	Upper W-flank	2°45.760	35°54.662
OL 503	Lengai I	Phonolite	Lower E-flank	2°45.402	35°57.447
OL 226	Lengai I	Phonolite	Upper S-flank	2°45.953	35°54.953
OL 440	Lengai I	Phonolite	Lower SE-flank	2°46.532	35°56.453
OL 795	Lengai I	Phon-neph	Upper S-flank	2°45.936	35°55.167
OL 801	Lengai IIA	CWN	Upper N-flank	2°45.128	35°54.942
OL 803	Lengai IIA	CWN	Upper N-flank	2°45.167	35°54.964
OL 789	Lengai IIA	CWN	Upper N-flank	2°45.081	35°54.704
OL 7/88	Lengai IIB	CWN	Upper NW-flank	2°45.485	35°54.693
OL 230	Lengai IIB	CWN	Upper NW-flank	2°45.391	35°54.642
OL 788	Lengai IIB	CWN	Upper N-flank	2°45.101	35°54.760
OL 802	Lengai IIB	CWN	Upper N-flank	2°45.128	35°54.942
OL 804	Lengai IIB	CWN	Upper N-flank	2°45.167	35°54.964
OL 806	Lengai IIB	CWN	Upper E-flank	2°45.812	35°55.222
OL 642	Lengai IIB	CWN	Fissure S of Nasira parasitic cones	2°43.402	35°55.123
OL 184	Lengai II	Mel-CWN	Northern Nasira parasitic cone	2°42.755	35°55.248
OL 247	Lengai II	Mel-CWN	Lower NE-flank, Dorobo canyon	2°44.078	35°57.012

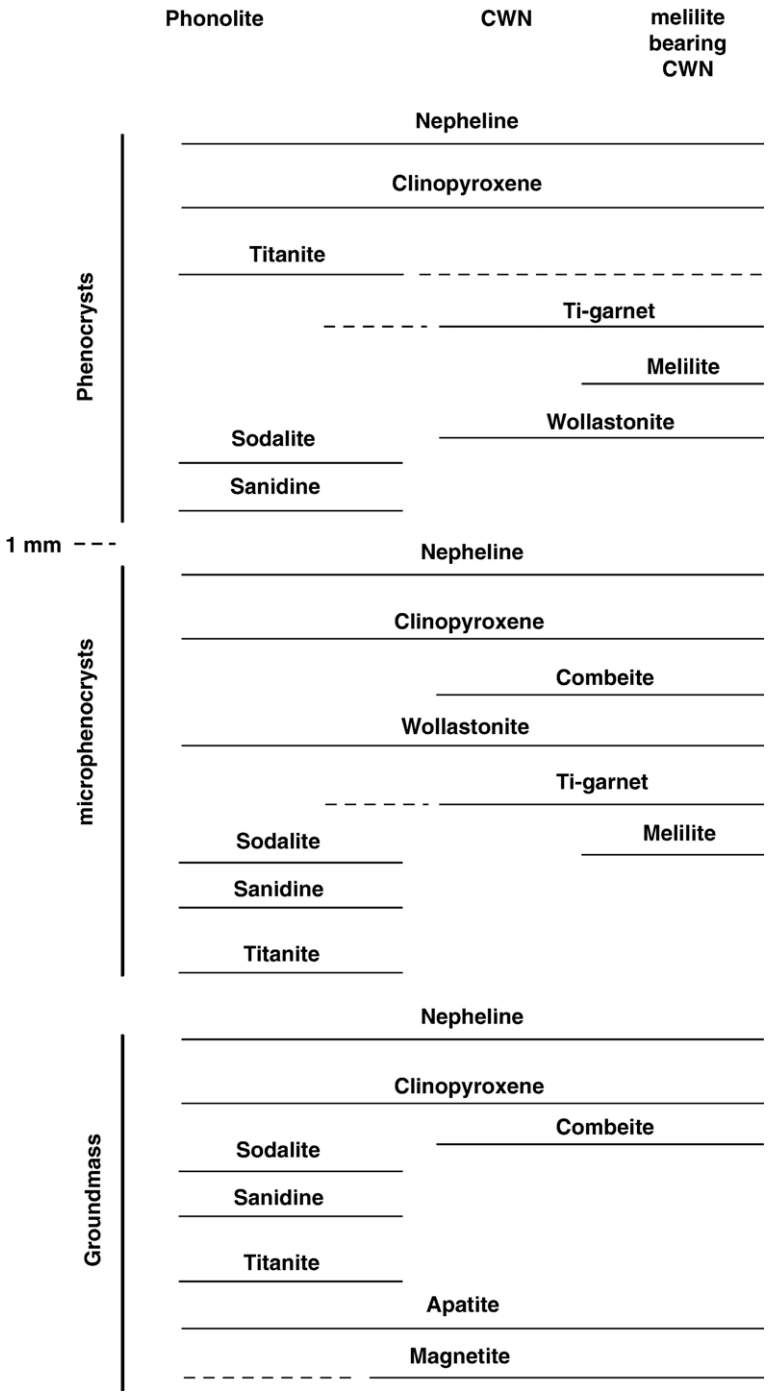

Fig. 3. Variations in mineral association in Oldoinyo Lengai peralkaline lavas; dashed lines indicate that the mineral is less abundant.

Stratigraphic relations do not allow correlation of OL247 sample to subunits within Lengai II. Four different textural types of combeite can be found: phenocrysts reaching 700 μm in diameter, coronas around wollastonite and clinopyroxene (also described by Dawson et al., 1989) and globular patches of combeite (see also Donaldson et al., 1987), which we interpret as complete replacement of wollastonite. Wollastonite can also be replaced by calcite. Alteration of combeite enhances symmetrical and concentric

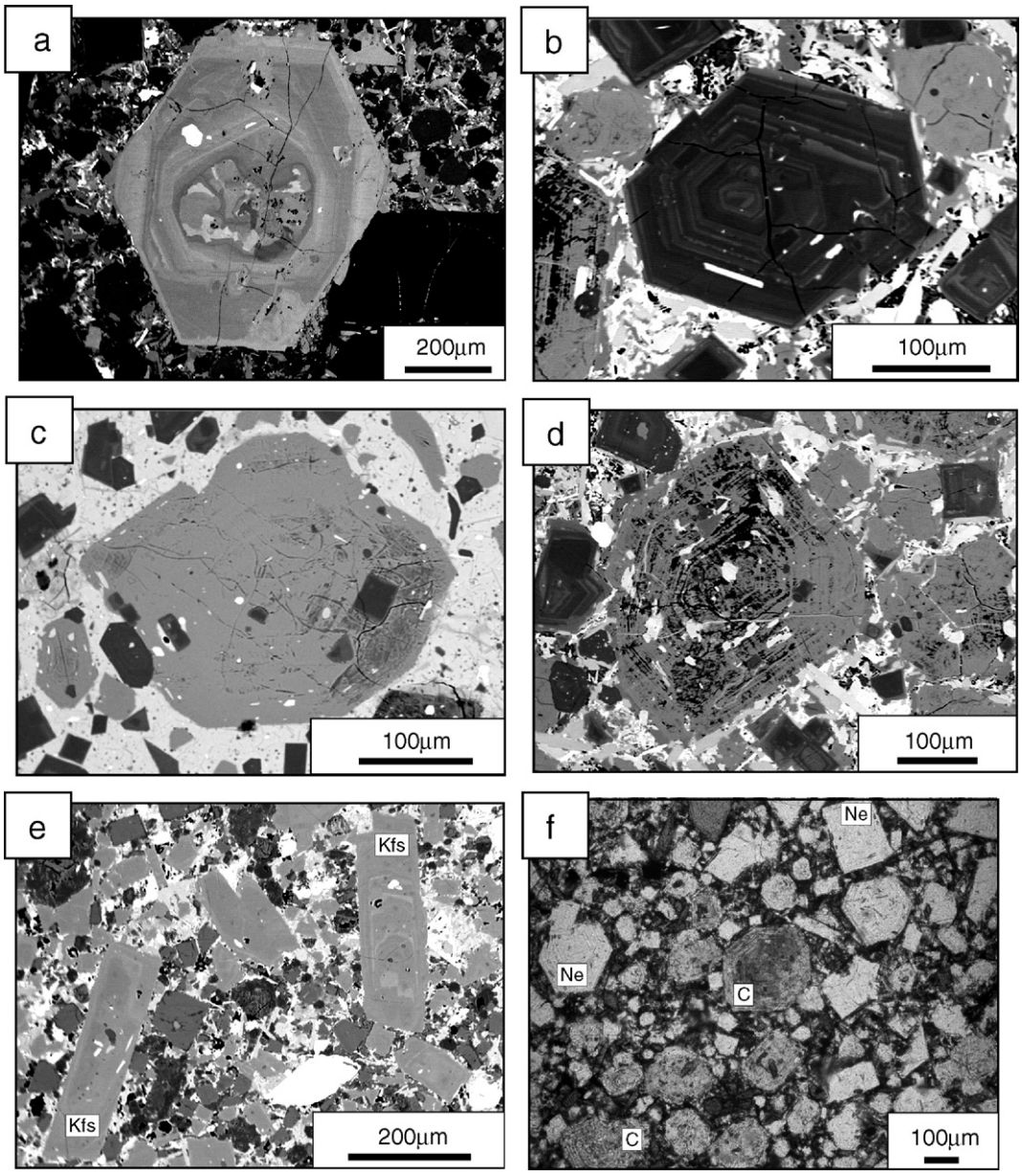

Fig. 4. Back-scattered electron images of mineral phases in Oldoinyo Lengai lavas (a–e) and plane polarized light image of groundmass in OL 804 (f). (a) Zoned phenocryst of clinopyroxene in microcrystalline groundmass OL 804 showing corroded patchy core and several zones of overgrowth. For analyses see Table 4. (b) Oscilatory zoned phenocryst of nepheline in microcrystalline groundmass OL 804 with aligned inclusions of Cpx. Bright zones contain more iron than dark zones. For analyses see Table 4. (c) Fresh phenocryst of combeite in glassy matrix OL 803 with inclusions of nepheline and Cpx. (d) Altered phenocryst of combeite in microcrystalline groundmass OL 804 with inclusions of Cpx and nepheline. Alteration enhances oscillatory zoning. (e) Tabular zoned phenocrysts of sanidine (Kfs) in microcrystalline groundmass OL 822. Other phenocryst phases are nepheline, sodalite, Cpx and titanite. (f) Groundmass crystals of nepheline (Ne), combeite (C) and Cpx. Note amount of combeite (~50%).

optical zoning (Fig. 4d). Sector twinning is common in less altered grains. Combeite always contains inclusions of groundmass phases such as nepheline, clinopyroxene, Ti-garnet and apatite, pointing to fast late-stage crystallization (Fig. 4c, d). In the most evolved lava samples (e.g. OL804) combeite displays almost 50 modal% of the groundmass (Fig. 4f). Some Lengai II samples contain glomerophyric aggregates with euhedral nepheline, Ti-garnet, clinopyroxene and apatite. These aggregates are mineralogically similar to plutonic blocks (Dawson et al., 1995), but often show interstitial green glass.

5. Whole rock geochemistry

5.1. Major elements

Chemical analyses of 21 Oldoinyo Lengai cone lava samples are given in Table 1. The TAS diagram (Le Maitre et al., 1989) is used (Fig. 5) to classify the silicate lavas. Lavas from unit Lengai I form a distinct area in the phonolite field and samples from unit Lengai II plot in the foidite field. They are separated at a SiO_2 content of 49 wt.%. Lava sample OL795 from Lengai I displays a small overlap with the nephelinite field. This sample shows chemical and mineralogical similarities with Lengai II CWN samples. It belongs to Lengai I, sampled at the upper southern slope approximately 50 m below the southern crater rim. Phonolite of Lengai I are restricted to total alkali contents ranging between 14 and 17 wt.%. Lengai II samples are exclusively CWN and minor melilite bearing CWN and vary from about 15 to 21 wt.% total alkalis (Na_2O+K_2O). In general, Lengai II A lavas show lower total alkali values than Lengai II B lavas, which indicates increasing peralkalinity with time. The melilite-bearing CWN OL247 and OL184 extend the field of Lengai II lavas and are the most undersaturated samples found in this unit. A similar pattern can be observed in the SiO_2 vs. peralkalinity index ((Na+K)/Al) diagram (Fig. 6a). All Lengai I and II samples plot above the value of 1, which defines peralkaline rocks. A maximum peralkalinity index value of 2.36 was found in sample OL802. As in the TAS diagram, OL624 from the Nasira parasitic cones plots close to the CWN of Lengai II B.

Overall, the ultrabasic to basic silicate lavas from Oldoinyo Lengai show an evolved composition. Maximum MgO-contents of all published and available analyses (Donaldson et al., 1987; Dawson, 1989; Peterson, 1989a; Keller and Spettel, 1995; Dawson, 1998; this publication) do not exceed about 2 wt.% MgO (Fig. 6b) and all magnesium numbers Mg#=100Mg/(Mg+Fe^{2+}) with Fe^{2+} calculated as Fe_2O_3/FeO=0.15 are below or well below 30. The highly fractionated nature is underlined by Ni and Cr-contents that are consistently ≤10 ppm as well as by the generally enriched incompatible element patterns.

A marked increase in iron, calcium, sodium, and manganese is observed from Lengai I phonolite to and within Lengai II CWN and mel-CWN (Fig. 7). At the same time Al_2O_3 decreases, while TiO_2-contents remain constant around 1 wt.%, K_2O around 5 wt.% and P_2O_5 around 0.4 wt.%.

A large compositional gap separates Lengai II CWN from the primitive olivine melilitite and olivine-

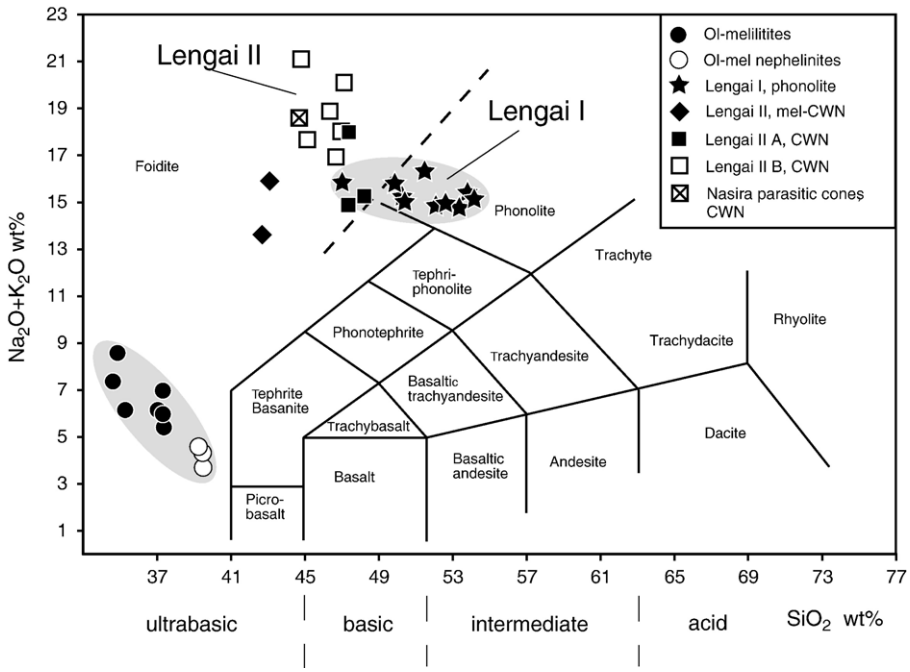

Fig. 5. TAS-diagram after Le Maitre et al. (1989) for Oldoinyo Lengai peralkaline lavas. Dashed line denotes proposed division between Foidite and Phonolite fields. Olivine melilitite and olivine-melilite nephelinite data from Keller et al. (2006-this volume).

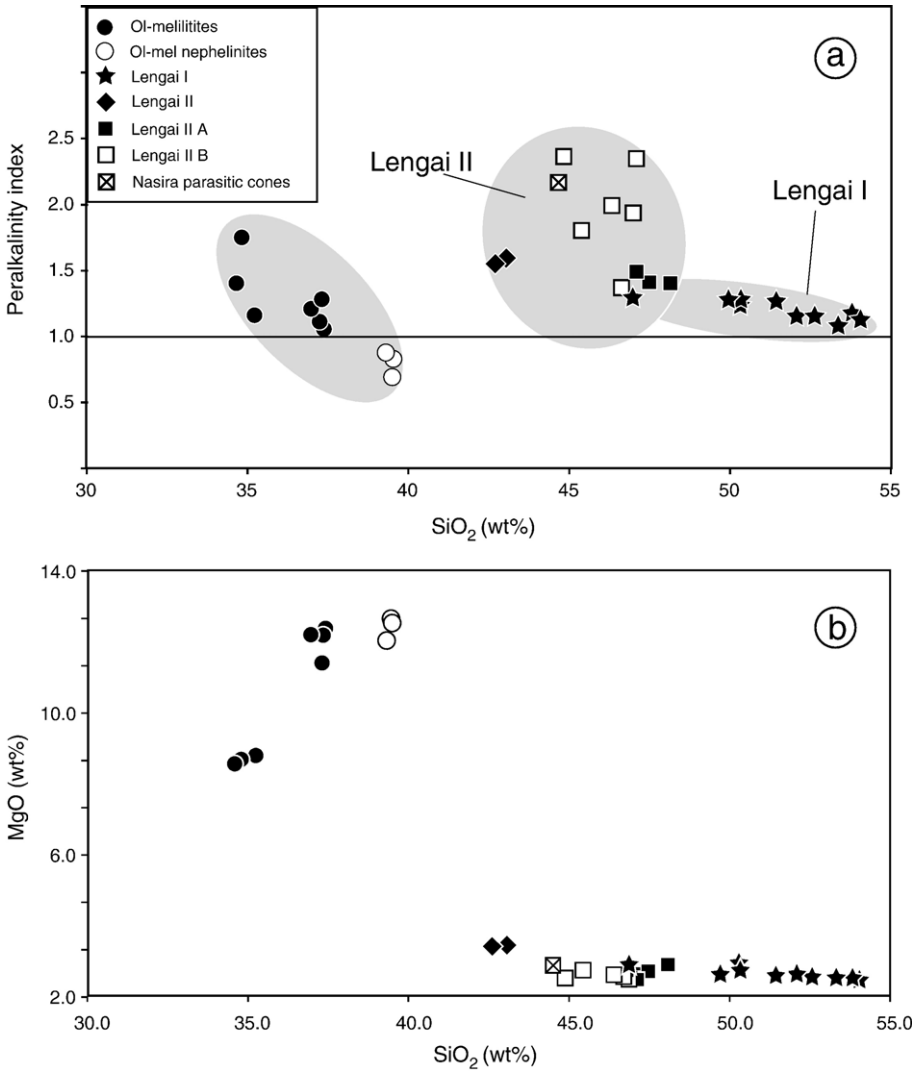

Fig. 6. (a) SiO_2 vs. peralkalinity index for Oldoinyo Lengai peralkaline lavas. (b) SiO_2 vs. MgO relationship for Oldoinyo Lengai peralkaline lavas. Symbols as in Fig. 5. Olivine melilitite and olivine-melilite nephelinite data from Keller et al. (2006-this volume).

melilite nephelinites (Keller et al., 2006-this volume). This gap exists in all Harker diagrams (Fig. 7) but is best visible in the MgO vs. SiO_2-plot (Fig. 6b). Although Peterson and Kjarsgaard (1995) proposed olivine melilitite as the parental melt for the genesis of CWN, no intermediate members that plot in this gap have been found at Oldoinyo Lengai. An assumed relationship by fractionation remains hypothetical. Moreover, Keller et al. (2006-this volume) discuss differences in radiogenic isotope ratios between the olivine melilitites and the silicate lavas of the cone. In addition, phonolites and CWNs of Lengai II form separate groups in the Sr–Nd isotope system (Bell and Dawson, 1995).

5.2. Trace elements and REE

Trace elements for silicate lavas of Oldoinyo Lengai are reported in Table 1 while REE and additional trace elements are listed in Table 2. Donaldson et al. (1987) provide selected trace element data for 12 samples and REE data for 5 samples within the stratigraphy of Dawson (1962). Peterson (1989a) reported trace elements for 6 of the samples designated as WN (wollastonite nephelinite) and CN (combeite nephelinite), but without geologic or stratigraphic location and context. Keller and Spettel (1995) used the Recent "rim lava" at the western crater rim (OL 7) as a combeite–wollastonite nephelinite reference for the discussion of

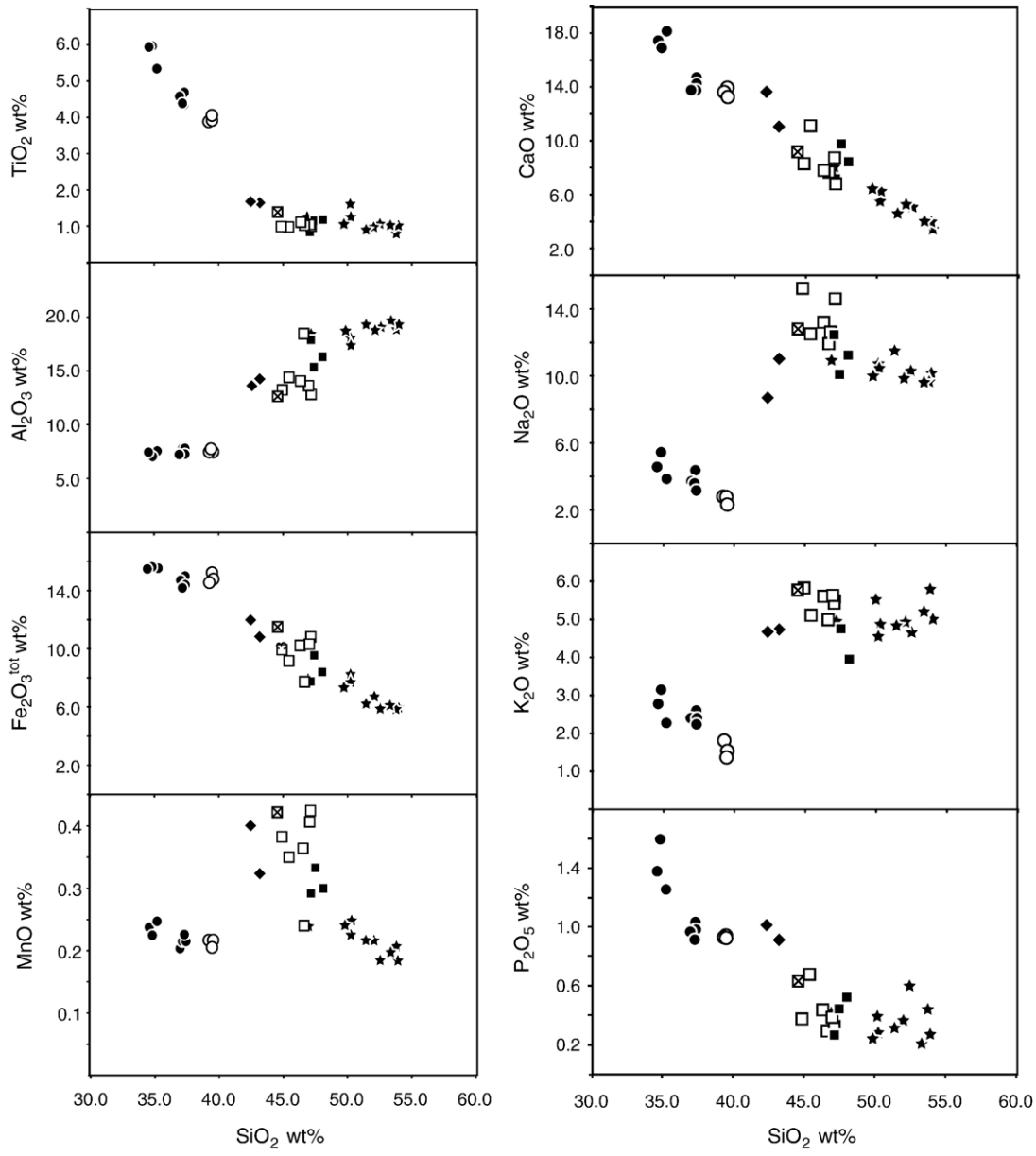

Fig. 7. Harker diagrams for Oldoinyo Lengai peralkaline lavas. Symbols as in Fig. 5. Olivine melilitite and olivine-melilite nephelinite data from Keller et al. (2006-this volume).

relationships between silicate lavas and natrocarbonatite at Oldoinyo Lengai. Dawson (1998) provides trace element data for three additional samples.

Characteristics shared by both major lava groups, the Lengai I phonolite and the Lengai II CWN, include low concentrations of compatible elements (Ni, Cr, Co, etc.) reflecting the fractionated nature of cone lavas (Donaldson et al., 1987). Incompatible elements are enriched and show increasing concentrations from phonolite to CWN, e.g. Sr from 1844 ppm in phonolite to 2427 ppm in CWN, Rb from 97 ppm to 104 ppm, Ba from 1462 ppm to 1892 ppm and Zr from 539 ppm to 782 ppm. Similarly, Nb, Y, Hf, Th and Ta are high in CWN. Average Th-concentrations are higher in phonolite than in CWN (24.4 ppm vs. 13.1 ppm, respectively).

Incompatible elements are enriched up to 750 times with regard to mantle averages (Sun and McDonough, 1989). Significant positive anomalies are noticeable for Th, U, Pb and Zr and negative anomalies for P, Sm and Ti (Fig. 8a). Patterns of mantle-normalized incompatible

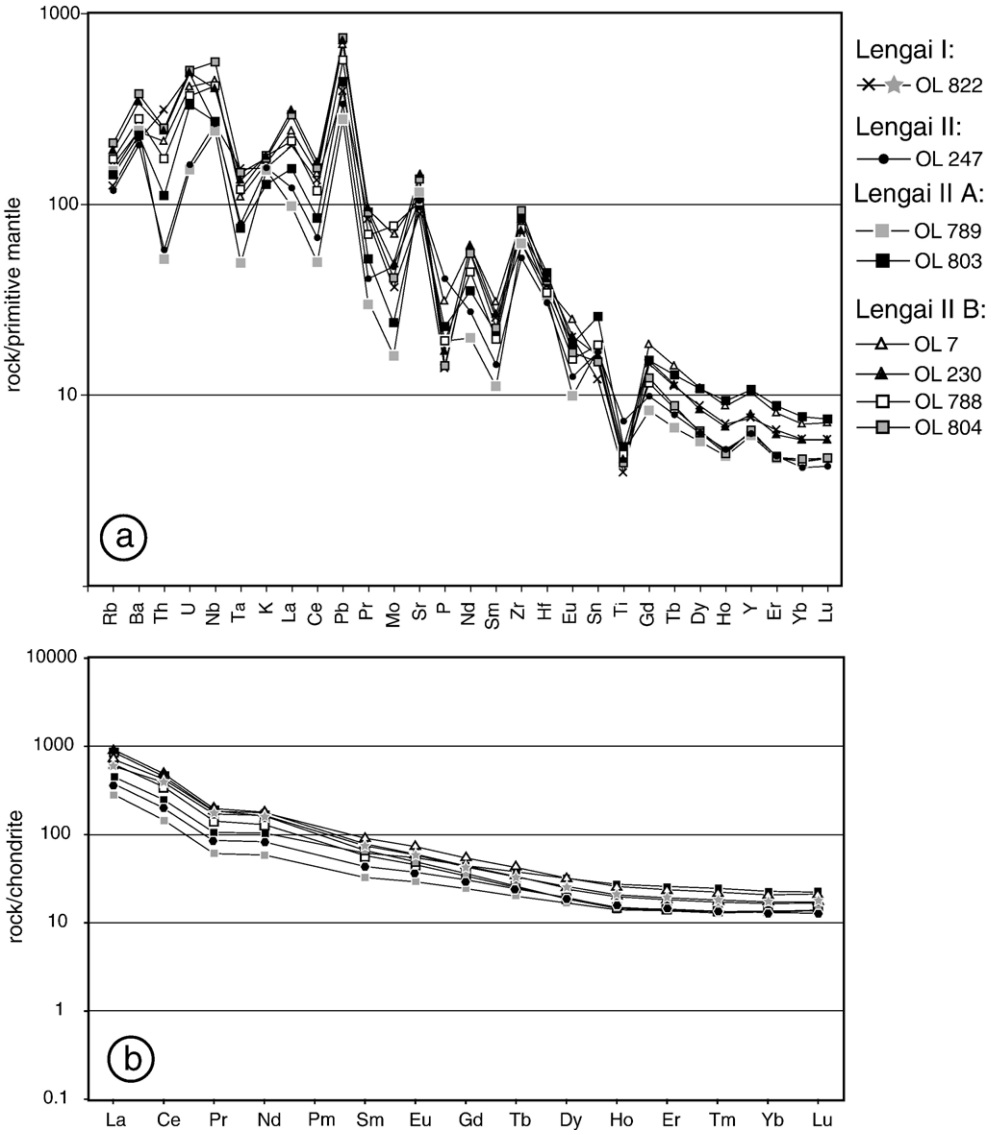

Fig. 8. (a) Primitive mantle-normalized incompatible trace element abundances in Oldoinyo Lengai peralkaline lavas. (b) Chondrite-normalized REE diagramm. Normalizing values from McDonough and Sun (1995), OL 7 data from Keller and Spettel (1995).

element abundances (Fig. 8a) and REE (Fig. 8b) show marked enrichment in LREE and are similar in phonolite and CWN.

LREE are up to 906 times chondritic. La/Yb_{CN} and La/Sm_{CN} ratios are 34.6 and 8.1 for phonolite and 39.3 and 10.0 for CWN, respectively. The previously known REE distribution pattern for the 1917-rim lava (CWN OL7; Keller and Spettel, 1995) is confirmed by the larger data set presented here. The patterns in the chondrite-normalized diagram (Fig. 8b) are very similar for phonolite and CWN.

Th/U ratios are 2.6 to 5.5 in phonolite, and 1.1–3.6 in CWN. In general, incompatible element ratios such as Zr/Hf, Zr/Nb, Nb/Ta and Hf/Ta all increase from phonolite to CWN. Zr/Hf ratios range from 40 to 60 in phonolite. These ratios are slightly higher than the rather constant ocean island basalt (OIB) value of 36 (Sun and McDonough, 1989) and increase from 50 to 80 in CWN. Zr/Nb ratios range from 2.7 to 3.7 and from 2.6 to 4.8, respectively. Average Nb/Ta ratios are 25.6 in phonolite and 62.4 in CWN (using the ICP-MS data of Table 1) and Hf/Ta are 1.4–1.8 and 2–5, respectively. These values deviate from the typical OIB values of 17.7 for Nb/Ta and 2.9 for Hf/Ta (Sun and McDonough, 1989).

Ce/Pb ratios vary slightly from 4.5 to 8.4 in comparison to the constant OIB value of 25±5 (Sun

and McDonough, 1989). Primitive olivine melilitites (Keller et al., 2006-this volume) have ratios that are similar to OIB, while Ce/Pb is much lower in all peralkaline cone lavas of Lengai I and Lengai II. With values of 6.8 to 8.4 for phonolite and 4.5 to 5.8 for CWN (Tables 1 and 2), a slight but systematic difference between the two groups is noticeable.

In terms of incompatible element enrichment, the CWN group is more evolved than the phonolite group.

6. Mineral chemistry

For this study, nepheline and clinopyroxene were analyzed by electron microprobe since they represent the major mineral phases in lavas of the two cone-building units, Lengai I and Lengai II. In addition, we present data for combeite, which is an important mineral phase in CWN of Lengai II. From 21 lava samples, the least altered were selected for mineral analyses. These are OL822 (Lengai I), OL803 (Lengai II A), OL788 (Lengai II B) because of its "fresh" combeite and OL804 (Lengai II B) because of its evolved character.

6.1. Nepheline

Representative analyses of nepheline are listed in Table 4. Nepheline phenocrysts and even groundmass crystals in CWN are zoned. Zoning is most pronounced in nepheline of Lengai II B. In back scattered electron (BSE) images, phenocrysts show narrow oscillatory zoning patterns (Fig. 4b) and groundmass crystals show a narrow bright rim. Their Ne/Ks ratio

Table 4
Representative analyses of nepheline, combeite and clinopyroxene in Oldoinyo Lengai lavas

Analysis	1	2	3	4	5	6	7	8	9	10	11	12
Mineral	ne	ne	ne	com	com	com	cpx	cpx	cpx	cpx	cpx	cpx
wt.%												
SiO_2	41.36	44.79	40.55	50.15	50.43	50.81	50.66	49.24	50.31	52.04	50.73	50.96
TiO_2				0.08	0.04	0.06	0.85	1.17	0.39	0.53	0.38	0.55
Al_2O_3	32.93	30.32	26.18	0.03	0.03	0.02	1.18	1.18	0.46	0.72	0.82	0.92
Fe_2O_3*	1.37	3.31	10.28	8.98	1.36	1.39						
FeO*							10.55	21.66	21.01	10.73	19.13	19.00
MnO				1.26	0.45	0.39	0.35	0.49	0.90	0.38	0.60	0.54
MgO	0.02	0.12	0.19	0.22	0.15	0.14	12.26	5.19	5.58	12.15	6.49	6.48
CaO	0.08	0.02	0.01	14.12	25.6	26.36	23.05	16.26	18.51	22.46	18.00	17.17
Na_2O	15.47	17.21	14.74	24.31	21.44	21.28	1.06	4.64	3.13	1.50	3.65	4.03
K_2O	8.05	4.05	8.59	0.05	0.04	0.07	0.01	0.00	0.00	0.00	0.01	0.02
SrO				0.25	0.7	0.59						
Total	99.28	99.82	100.53	99.45	100.24	101.11	99.98	99.84	100.29	100.51	99.81	99.67
Cations per 4 oxygens				Cations per 9 oxygens			Cations per 6 oxygens					
Si	1.02	1.09	1.07	2.85	2.97	2.96	1.90	1.89	1.94	1.93	1.94	1.95
Ti				0.00	0.00	0.00	0.02	0.03	0.01	0.01	0.01	0.02
Al	0.96	0.87	0.82	0.00	0.00	0.00	0.05	0.05	0.02	0.03	0.04	0.04
Fe^{3+}	0.01	0.03	0.10	0.40	0.06	0.06	0.18	0.44	0.31	0.18	0.33	0.33
Fe^{2+}							0.15	0.25	0.37	0.15	0.28	0.27
Mn				0.06	0.02	0.02	0.02	0.02	0.03	0.02	0.02	0.02
Mg	0.00	0.00	0.01	0.02	0.01	0.01	0.68	0.30	0.32	0.68	0.37	0.37
Ca	0.00	0.00	0.00	0.86	1.62	1.65	0.92	0.67	0.77	0.89	0.74	0.70
Na	0.74	0.81	0.76	2.68	2.45	2.41	0.08	0.35	0.23	0.11	0.27	0.30
K	0.25	0.13	0.29	0.00	0.00	0.01	0.00	0.00	0.00	0.00	0.00	0.00
Sr				0.01	0.02	0.02						
Sum	2.98	2.93	3.05	6.88	7.15	7.14	4.00	4.00	4.00	4.00	4.00	4.00
			Na/(Na+Ca)	0.63	0.46	0.45 Cation%						
						Na	8.38	37.92	24.58	11.47	28.69	31.11
						Mg	74.53	32.65	33.66	71.19	39.29	38.49
						Fe^{2+}+Mn	17.09	29.43	41.76	17.35	32.03	30.40

1–3 Nepheline: 1 core of phenocryst OL 804, 2 groundmass grain OL 822, 3 rim of phenocryst OL 804; 4–6 combeite: 4 micro phenocryst OL 804, 5–6 micro phenocryst OL 788; 7–12 clinopyroxene: 7 phenocryst core OL 804, 8 bright zone of phenocryst OL 804, 9 phenocryst core OL 803, 10 dark zone of phenocryst OL 803, 11 phenocryst core OL 822, 12 phenocryst rim OL 822.
∗=Total Fe as Fe_2O_3 for nepheline and combeite, as FeO for clinopyroxene; for clinopyroxene, Fe^{2+} and Fe^{3+} were calculated assuming stoichiometry.

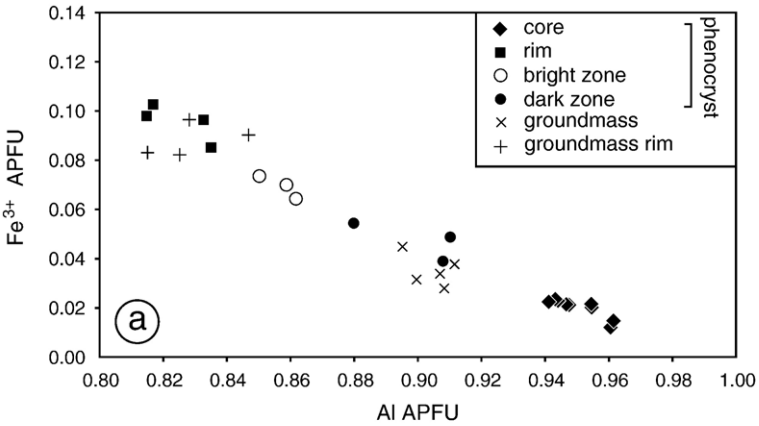
0.14
0.12
0.10
0.08
0.06
0.04
0.02
0.00
Fe3+ APFU
0.80
0.82
0.84
0.86
0.88
0.90
0.92
0.94
0.96
0.98
1.00
Al APFU
core
rim
bright zone
dark zone
groundmass
groundmass rim
phenocryst
a

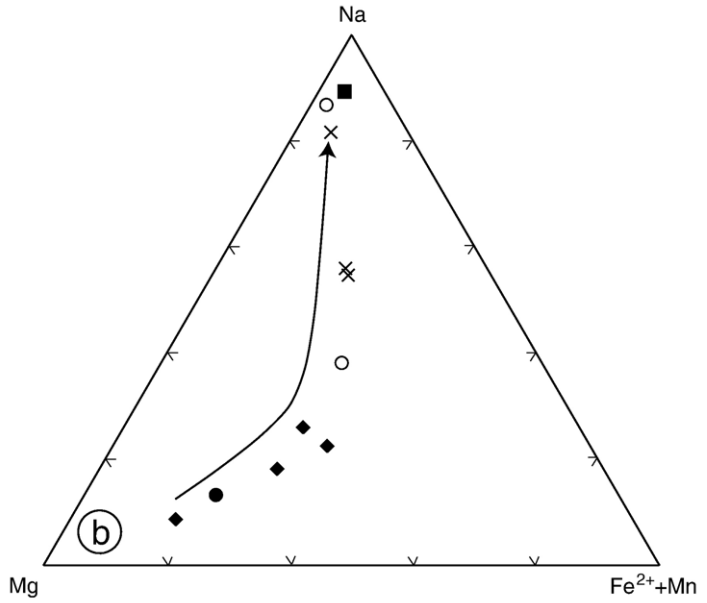
Na
Mg
Fe2+ +Mn
b

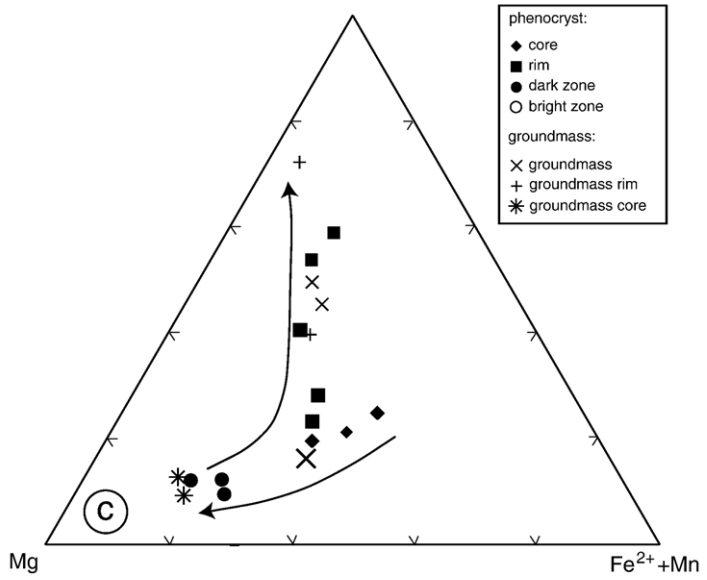
phenocryst:
core
rim
dark zone
bright zone
groundmass:
groundmass
groundmass rim
groundmass core
Mg
Fe2+ +Mn
c

varies from below 2 in Lengai II B CWN to 4.3 in Lengai I phonolite. The increasing Ne/Ks ratio in nepheline confirms results by Donaldson et al. (1987) who described increasing Ne/Ks ratios with increasing whole rock SiO_2-contents in Oldoinyo Lengai lavas. Minimum ratios reported here are lowest in sample OL804 CWN of Lengai II B. This sample is more SiO_2 rich (45.51 wt.%) than Donaldson's sample BD70 (44.13 wt.%). The most striking feature of Lengai II nepheline is an exceptionally high Fe^{3+}-content increasing from 3.31 wt.% Fe_2O_3 in Lengai I phonolite to 10.28 wt.% Fe_2O_3 in Lengai II B CWN. Fig. 9a shows a strong negative correlation between Fe^{3+} and Al. In general, increasing iron content in nepheline within the evolution of Lengai lavas can be explained by increasing whole-rock iron content and relatively oxidized crystallization conditions (Mann et al., 2006-this volume).

6.2. Combeite

Combeite can be expressed with the ideal formula $Na_2Ca_2Si_3O_9$ (Sahama and Hytönen, 1957). Representative analyses of combeite are listed in Table 4. Based on petrography, all analyses represent combeite of magmatic origin. Na-contents range from 20 to 24 wt.%, implying a Na excess of 0.3–0.7 atoms over the stoichiometric formula. Ca-contents cover a range from 14 to 26 wt.% and are under-represented in the stoichiometric formula by 0.4–1.1 atoms. Calculated Na/(Na+Ca) ratios vary from 0.45 to 0.63. Based on this ratio, Dawson (1998) distinguishes primary magmatic combeite (Na/(Na+Ca)=0.62–0.66) from secondary combeite (Na/(Na+Ca)=0.57–0.59; see Section 4). Although we did not analyze the latter type, our data imply that this ratio is not suitable to distinguish combeite types of different origin. The maximum Fe-content is particularly high with up to 8.98 wt.% Fe_2O_3. Sahama and Hytönen (1957) published a combeite analysis that includes Fe_2O_3 and FeO. Because Fe_2O_3 dominates, we calculated all Fe as Fe^{3+}, which leads to improved results in the structural formula for the given analyses. In addition, combeite contains Sr in minor amounts (up to 0.7 wt.% SrO). A more accurate structural formula for an iron-rich combeite from sample OL804 is $(Na_{2.68}Ca_{0.86}Fe_{0.40}Mn_{0.06}Sr_{0.02})Si_3O_9$. Contents for Na, Mn and especially Fe in OL804 of Lengai II B CWN extend the range of published combeite data (Sahama and Hytönen, 1957; Dawson et al., 1989; Peterson, 1989a; Keller and Krafft, 1990; Dawson and Hill, 1998; Dawson, 1998).

6.3. Clinopyroxene

In all samples, two generations of clinopyroxene are present: large phenocrysts and groundmass crystals. Representative analyses are listed in Table 4 where Fe^{3+} was calculated assuming stoichiometry. In all analyses Si+Al is <4, indicating a significant deficiency on the tetrahedral site. High Ti-contents along with excess Fe^{3+} over Na and a negative correlation between Si and Ti and Si and excess Fe^{3+} account for the presence of Ti and/or Fe^{3+} on the tetrahedral site in some of the analyses (Table 4). Clinopyroxenes are zoned in all lava types, most intensely in CWN. Fig. 9b and c show clinopyroxene analyses for two CWN in the Na–Mg–(Fe^{2+}+Mn) system. These clinopyroxene phenocrysts show a corroded, patchy core, several zones of oscillatory overgrowth (Fig. 4a) and narrow, deep bottle-green rims. The crystallization process of CWN clinopyroxene of Lengai II B shows a progressive trend towards Na-rich clinopyroxene covering a wide range of compositions (Fig. 9b). Whereas the cores and dark zones of phenocrysts are characterized by high amounts quadrilateral components, rims, groundmass crystals and the bright zones of phenocrysts are enriched in acmite-component. In CWN of Lengai II A, clinopyroxene crystallization starts with diopside- and hedenbergite-component values close to 40%. However, they do not reach such high values as in CWN of Lengai II B (Fig. 9c).

7. Discussion

Donaldson et al. (1987) distinguished nephelinite, phonolitic nephelinite and phonolite at Oldoinyo Lengai. With the recognition of combeite (and wollastonite) in Oldoinyo Lengai lavas (Dawson et al., 1989; Peterson, 1989a,b; Keller and Krafft, 1990) the Lengai II CWN became central in the petrogenetic discussion of Oldoinyo Lengai. On the basis of microscopic investigation all Lengai II lavas are combeite- and wollastonite-bearing and designated as CWN. In the following we will discuss the relationships between the proposed parental melts (olivine melilitite; Keller et al., 2006-this volume), the more evolved silicate

Fig. 9. (a) Fe^{3+}-atoms per formula unit vs. Al-atoms per formula unit for zoned nepheline in OL 804 CWN of Lengai II B. (b) and (c) Clinopyroxene composition in the Na–Mg–(Fe^{2+}+Mn) triangle. (b) OL 804 CWN of Lengai II B; (c) OL 803 CWN of Lengai II A. Lavas become less undersaturated from (b) to (c). Representative data are given in Table 4. Arrows indicate direction of progressive crystallisation.

lavas of the Oldoinyo Lengai cone (phonolite and CWN) and the natrocarbonatite.

7.1. Relationship between the parental melts and evolved lavas

Using major element data for rocks and minerals from this study (Tables 1 and 4) and from Keller et al. (2006-this volume) the total chemical variation of olivine melilite (Fig. 7) can be modeled by fractionation of up to 10% olivine and 6% melilite combined with the accumulation of 2% apatite and perowskite, respectively. However, the evolution from olivine melilite towards olivine nephelinite must be more complex and cannot be explained by fractionational crystallization alone. Also, neither phonolite nor CWN whole-rock compositions can be explained by fractionation from olivine melilite. Consequently, additional processes (assimilation of country rocks, mixing of different mantle components, liquid immiscibility or exsolution of fluid phases) need to be involved, which is consistent with isotope data compiled in Keller et al. (2006-this volume).

7.2. Phonolite–CWN relationship

CWN and phonolite are the silicate lavas of the Oldoinyo Lengai cone. Phonolite of primordial Lengai I and CWN of Lengai II share several geochemical similarities. Both groups are peralkaline and show similar LILE and REE patterns, but are isotopically distinct (Bell and Dawson, 1995; Bell and Tilton, 2001). It appears that phonolite and CWN evolved along different paths, either from distinct parental melts (Peterson and Kjarsgaard, 1995) or from a common parental melt under different physico-chemical conditions. The chemical and mineralogical variation between Lengai IIA and IIB CWN can be modeled by fractionation of diopside (5%) and titanite (6%) and by the accumulation of aegirine (22%), combeite (18%) and Ti-garnet (6%). Within phonolite, estimated fractionation of wollastonite (6%) and nepheline (13%) and accumulation of sanidine (7%) explain the observed variation in whole-rock data.

In the Sr/Nd-isotope system, two types of nephelinite are distinguished, Group I and Group II (Bell and Dawson, 1995; Bell and Simonetti, 1996; Dawson, 1998). Wollastonite nephelinite, combeite–wollastonite nephelinite and combeite nephelinite form Group I. This group, the CWN of this paper, is represented by the Lengai II lavas of the northern crater and cone. The Group II nephelinite samples analyzed by Donaldson et al. (1987) are stratigraphically less well constrained, because three of the four samples were ejected blocks. With lava sample BD64, collected at the southern wall of the Eastern Chasm (J.B. Dawson pers. com.), a sector collapse scar in the eastern flank, it appears that Group II nephelinite are older than Group I and belong stratigraphically together with phonolite to the Lengai I unit. The Sr/Nd-isotope system indicates complex mixing of several components (Bell and Dawson, 1995; Bell and Tilton, 2001; Keller et al., 2006-this volume). Further constraints on this isotopic grouping are expected from a systematic isotope study, which is in progress.

7.3. CWN–carbonatite relationship

In terms of stratigraphy, CWN and natrocarbonatite are closely related to each other, where natrocarbonatite is the most recent product. Isotopically, Lengai II CWN and natrocarbonatite are almost identical (Keller and Krafft, 1990; Bell and Dawson, 1995).

In this paper it is shown that all Lengai II lavas are combeite-bearing. Dawson (1998) argues that natrocarbonatite at Oldoinyo Lengai separated from wollastonite nephelinite after combeite crystallization, with combeite reaction rims around wollastonite and clinopyroxene being the evidence. In this study we show that Na/(Na+Ca)-values of magmatic combeite incorporate the values of these combeite reaction rims.

The effects of an assumed separation of natrocarbonatite from CWN by liquid immiscibility should include an increase in SiO_2, FeO, MnO, Al_2O_3, MgO, TiO_2 in the latter. Trace element partitioning data of Veksler et al. (2005) show that Zr, Hf, and the HREE fractionate into the conjugate silicate melt. At the same time Na_2O, CaO, Sr, Ba, and the LREE, should decrease because they preferentially fractionate into the natrocarbonatite melt (Keller and Spettel, 1995; Kjarsgaard et al., 1995; Dawson, 1998; Veksler et al., 2005). Our data does not show a clear pattern in this respect. Possibly the percentage of immiscible carbonatite melt is so low that the described effects are not observed in our data. A candidate to display the conjugate silicate liquid is the melilite-bearing CWN. This composition is low in Na, Sr and Ba compared to melilite-free CWN.

8. Summary

CWN are mineralogically and geochemically unusual and unique at Oldoinyo Lengai, where they represent the dominant magma composition of Lengai II. They were erupted during a major cone building stage following a north-directed sector collapse of a phonolitic

edifice. Lengai I phonolite and Lengai II CWN form chemical distinct groups that are not linked genetically to each other in a simple manner. Petrography of lava samples from the northern cone shows that nephelinite is combeite and wollastonite-bearing. Within the volcano's temporal evolution, phonolite and nephelinite show a distinct trend to more silica undersaturated compositions and increasing peralkalinity, especially within the CWN of Lengai II. This trend is manifested in several ways including the appearance of combeite, a Na–Ca phase without Al in its structure, an indicator for high peralkalinity. The complex zoning patterns of clinopyroxene and nepheline document the crystallization history of the lavas. Na and Fe-contents in clinopyroxene and Fe in nepheline record the peralkaline evolution of the magma. The Fe^{3+}-contents in nepheline phenocryst rims and combeites are exceptionally high with a maximum at 10.28 wt.% and 8.98 wt.%, respectively. The chemical zonation of clinopyroxenes in Lengai II B CWN points to fractional crystallization processes that include Ca- and Mg-bearing phases such as diopside and Ti-garnet. Combeite, rims of clinopyroxene phenocrysts and clinopyroxene groundmass crystals reflect Fe-enrichment during the crystallisation of Lengai II CWN magma prior to eruption in contrast to the phonolite magma of Lengai I, which evolved over a smaller range.

Trace element and REE data show that Lengai II CWN is more evolved than Lengai I phonolite.

The petrogenetic connection of the evolved peralkaline silicate lavas of Oldoinyo Lengai to primary olivine melilitite and to the exceptional natrocarbonatite remains to be traced. But it seems plausible that olivine melilitite evolves due to fractional crystallization to form peralkaline CWN.

Acknowledgements

Thomas Finkenbein, Florian Neukirchen and Daniel Wiedenmann from IMPG Freiburg, the Dorobo organisation Arusha, Chris Weber of VEI, Tanzannature Arusha, Kidemi Kodomo and Burra Ami Gadiye from Engare Sero provided assistance in the field. We also thank Anatoly N. Zaitsev and Michael Marks for fruitful and pleasant exchange of ideas and results. ICP-MS data for trace elements were obtained through Jacques Morel and Laurin Sewes of CRPG-CNRS Nancy, France. Hiltrud Müller-Sigmund and Isolde Schmidt from IMPG Freiburg are thanked for their assistance at the electron microprobe and XRF, respectively. Paul Hoskin and Rodney Grapes read an early draft of the manuscript and gave valuable suggestions. Claus Siebe and John A. Wolff are thanked for a careful review and Gregor Markl for his editorial guidance. The Deutsche Forschungsgemeindschaft (DFG) has generously funded research under project KE 136/40.

References

Anderson, H., 2005. Young Explorers survey Tanzanian volcano—Ol Doinyo Lengai. Leica Geosystems. Customer Magazine. Reporter No. 52. February 2005. http://www.leica-geosystems.com/corporate/en/news/lgs_9134.htm.

Bagdasaryan, G.P., Gerasimovskiy, V.I., Polyakov, A.I., Gukasyan, R. K., Vernadskiy, V.I., 1973. Age of volcanic rocks in the rift zones of East Africa. Geochemistry International 10, 66–71.

Bell, K., Dawson, J.B., 1995. Nd and Sr isotope systematics of the active Carbonatite Volcano, Oldoinyo Lengai. In: Bell, K., Keller, J. (Eds.), Carbonatite Volcanism, Oldoinyo Lengai and the Petrogenesis of Natrocarbonatites. IAVCEI Proceedings in Volcanology, vol. 4. Springer Verlag, Berlin, pp. 100–112.

Bell, K., Simonetti, A., 1996. Carbonatite magmatism and plume activity: implications from the Nd, Pb and Sr isotope systematics of Oldoinyo Lengai. Journal of Petrology 37, 1321–1339.

Bell, K., Tilton, G.R., 2001. Nd, Pb and Sr isotopic compositions of east African carbonatites: evicence for mantle mixing and plume inhomogeneity. Journal of Petrology 42, 1927–1945.

Church, A.A., Jones, A.P., 1995. Silicate–carbonate immiscibility al Oldoinyo Lengai. Journal of Petrology 36, 869–889.

Dawson, J.B., 1962. The geology of Oldoinyo Lengai. Bulletin of Volcanology 24, 349–387.

Dawson, J.B., 1989. Sodium carbonate lavas from Oldoinyo Lengai, Tanzania: implications for carbonatite complex genesis. In: Bell, K. (Ed.), Carbonatites—Genesis and Evolution. Unwin Hyman, London, pp. 255–277.

Dawson, J.B., 1992. Neogene tectonics and volcanicity in the North Tanzania sector of the Gregory Rift Valley: contrasts with the Kenya sector. Tectonophysics 204, 81–92.

Dawson, J.B., 1998. Peralkaline Nephelinite–Natrocarbonatite Relationships at Oldoinyo Lengai, Tanzania. Journal of Petrology 39, 2077–2094.

Dawson, J.B., Hill, P.G., 1998. Mineral chemistry of a peralkaline combeitelamprophyllite nephelinite from Oldoinyo Lengai, Tanzania. Mineralogical Magazine 62, 179–196.

Dawson, J.B., Smith, J.V., Steele, I.M., 1989. Combeite ($Na_{2.33}Ca_{1.74-others_{0.12}}$)$Si_3O_9$ from Oldoinyo Lengai, Tanzania. Journal of Geology 97, 365–372.

Dawson, J.B., Smith, J.V., Steele, I.M., 1995. Petrology and mineral chemistry of plutonic igneous xenoliths from the carbonatite volcano, Oldoinyo Lengai, Tanzania. Journal of Petrology 36, 797–826.

Dawson, J.B., Pyle, D.M., Pinkerton, H., 1996. Evolution of natrocarbonatite from a wollastonite nephelinite parent: evidence from the June, 1993 Eruption of Oldoinyo Lengai, Tanzania. Journal of Geology 104, 41–54.

Donaldson, C.H., Dawson, J.B., Kanaris-Sotiriou, R., Batchelor, R.A., Walsh, J.N., 1987. The silicate lavas of Oldoinyo Lengai, Tanzania. Neues Jahrbuch für Mineralogie. Abhandlungen 156, 247–279.

Foster, A., Ebinger, C., Mbede, E., Rex, D., 1997. Tectonic development of the northern Tanzanian sector of the East African

Rift System. Journal of the Geological Society (London) 154, 689–700.

Keller, J., Krafft, M., 1990. Effusive natrocarbonatite activity of Oldoinyo Lengai, June 1988. Bulletin of Volcanology 52, 629–645.

Keller, J., Spettel, B., 1995. The trace element composition and petrogenesis of natrocarbonatites. In: Bell, K., Keller, J. (Eds.), Carbonatite Volcanism: Oldoinyo Lengai and the Petrogenesis of Natrocarbonatites. IAVCEI Proceedings in Volcanology, vol. 4. Springer Verlag, Berlin, pp. 70–86.

Keller, J., Zaytsev, A., Wiedenmann, D. 2006-this volume. Primary magmas at Oldoinyo Lengai: the role of olivine melilitites. Lithos 91, 150–172. doi:10.1016/j.lithos.2006.03.014.

Kjarsgaard, B.A., Hamilton, D.L., Peterson, T.D., 1995. Peralkaline nephelinite/carbonatite liquid immiscibility: comparison of phase composition in experiments and natural lavas from Oldoinyo Lengai. In: Bell, K., Keller, J. (Eds.), Carbonatite Volcanism: Oldoinyo Lengai and the Petrogenesis of Natrocarbonatites. IAVCEI Proceedings in Volcanology, vol. 4. Springer Verlag, Berlin, pp. 163–190.

Klaudius, J., Keller, J., 2004. Quaternary debris avalanche deposits at Oldoinyo Lengai, Tanzania. IAVCEI General Assembly, Pucon, Chile. Abstract.

Lee, W.J., Wyllie, P.J., 1994. Experimental data bearing on liquid immiscibility, crystal fractionation, and the origin of calciocarbonatites and natrocarbonatites. International Geology Review 36, 797–819.

Lee, W.J., Wyllie, P.J., 1998. Processes of crustal carbonatite formation by liquid immiscibility and differentation, elucidated by model systems. Journal of Petrology 39, 2005–2015.

Le Maitre, R.W., Bateman, P., Dudek, A., Keller, J., Lameyre, J., Le Bas, M.J., Sabine, P.A., Schmid, R., Sorensen, H., Streckeisen, A., Woolley, A.R., Zanettin, B., 1989. A Classification of Igneous Rocks and Glossary of terms: Recommendations of the International Union of Geological Sciences Subcommission on the Systematics of Igneous Rocks. Blackwell Scientific Publications, Oxford, UK.

Macdonald, R., Rogers, N.W., Fitton, J.G., Black, S., Smith, M., 2001. Plume–lithosphere interactions in the generation of the basalts of the Kenya rift, East Africa. Journal of Petrology 42, 877–900.

Mann, U., Marks, M., Markl, G. 2006-this volume. Influence of oxygen fugacity on mineral compositions in peralkaline melts: The Katzenbuckel volcano, Southwest Germany. Lithos 91, 262–285. doi:10.1016/j.lithos.2005.09.004.

McDonough, W.F., Sun, S.S., 1995. Composition of the Earth. Chemical Geology 120, 223–253.

Peterson, T.D., 1989a. Peralkaline nephelinites: I. Comparative petrology of Shombole and Oldoinyo L'engai, East Africa. Contributions to Mineralogy and Petrology 101, 458–478.

Peterson, T.D., 1989b. Peralkaline nephelinites: II. Low pressure fractionation and the hypersodic lavas of Oldoinyo Lengai. Contributions to Mineralogy and Petrology 102, 336–346.

Peterson, T.D., 1990. Petrology and genesis of natrocarbonatite. Contributions to Mineralogy and Petrology 105, 143–155.

Peterson, T.D., Kjarsgaard, B.A., 1995. What are the parental magmas at Oldoinyo Lengai? In: Bell, K., Keller, J. (Eds.), Carbonatite Volcanism: Oldoinyo Lengai and the Petrogenesis of Natrocarbonatites. IAVCEI Proceedings in Volcanology, vol. 4. Springer Verlag, Berlin, pp. 70–86.

Pouchou, J.L., Pichoir, F., 1991. Quantitative analysis of homogeneous and stratified microvolumes applying the model "PAP". In: Heinrich, K.F.J., Newbury, D.E. (Eds.), Electron Probe Quantitation. Plenum Press, New York, pp. 31–75.

Sahama, T.G., Hytönen, M.A., 1957. Götzenite and combeite, two new silicates from the Belgian Congo. The Mineralogical Magazine 31, 503–510.

Simonetti, A., Bell, K., Shrady, C., 1997. Trace and rare-earth-element geochemistry of the June 1993 natrocarbonatite lavas, Oldoinyo Lengai (Tanzania). Implications for the origin of carbonatite magmas. Journal of Volcanology and Geothermal Research 75, 89–106.

Smith, M., Mosley, P., 1993. Crustal heterogeneity and basement influence on the development of the Kenia rift, East Africa. Tectonics 12, 591–606.

Sun, S.S., McDonough, W.F., 1989. Chemical and isotopic systematics of oceanic basalts; implications for mantle composition and processes. In: Saunders, A.D., Norry, M.J. (Eds.), Magmatism in the Ocean Basins. Geological Society of London, London, pp. 313–345.

Veksler, I.V., Dorfmann, A., Dingwell, D.B., Dulski, P., Jeffries, T.E., 2005. Experimental study of element partitioning between silicate and carbonate immiscible liquids. Peralk, Workshop on peralkaline rocks, Tübingen. Abstract.

Wiedenmann, D., 2004. Vulkanologische Stellung und petrologische Interpretation der Biotit–Pyroxen–Olivin–Tuffe am Oldoinyo Lengai, Tansania. Diploma thesis, Freiburg. 89 pp.

Williams, R.W., Gill, J.B., Bruland, K.W., 1986. Ra–Th disequilibria systematics: timescale of carbonatite magma formation at Oldoinyo Lengai volcano, Tanzania. Geochimica et Cosmochimica Acta 50, 1249–1259.